Indian Journal of Chemical Technology
Vol. 29, November 2022, pp. 753-759
DOI: 10.56042/ijct.v29i6.67384

Silver ferrite embellished graphene oxide heterogenous nanocomposite for efficient electrochemical detection of gallic acid

E Murugan*, M Kaviya Sri, K Janakiraman, S Saranya, F Lyric & N Sathyabarata Sahoo
Department of Physical Chemistry, School of Chemical Science, University of Madras, Guindy Campus, Chennai 600 025, India
E-mail: dr.e.murugan@gmail.com

Received 19 August 2022; accepted 21 October 2022

Ferrites have attracted the research community owing to their invincible properties corresponding to their magnetic recoverability, recycling efficacy, and environmentally friendly behaviour. They are gaining importance in catalysis, sensors, supercapacitors, batteries, magnetic tunnel ferrofluids, magnetic drug delivery, and information storage. By taking advantage of ferrites, in this study, we have developed a silver ferrite embellished graphene oxide ($AgFe_2O_4$/GO) nanocomposite by decorating $AgFe_2O_4$ on graphene oxide (GO) by a viable route. The crystal structure, size, morphology, and magnetic behaviour of the fabricated nanocomposites have been investigated with the assistance of fourier transform infrared (FTIR) spectroscopy, RAMAN spectroscopy, X-ray diffraction, and scanning electron microscopic (SEM) techniques. The composite has been examined for the electrocatalytic determination of gallic acid (GA) by cyclic voltammetry and differential pulse voltammetry by its modification of glassy carbon electrode. This modified glassy carbon electrode has shown excellent electrocatalytic behaviour toward the detection of GA. These results can be used as an electrochemical standard in the estimation of total polyphenol content in the foodstuffs and extended to pharmaceutical and industrial applications.

Keywords: Cyclic voltammetry, Differential pulse voltammetry, Gallic acid, Polyphenol, Sensors, Silver ferrites

Spinel ferrites are widely used crystalline material with the chemical formula AFe_2O_4 (A=Mn, Co, Ni, Zn, Cu, Ag, Cd). They gain attention among researchers owing to their electrical conductivity, high thermal stability, recovering ability and eco-friendly nature[1, 2]. Spinel ferrites can be classified into three subclasses as mixed, normal, and inverse depending on the position of cations in the close packing structure which consist of 32 oxygen atom, 64 divalent tetrahedral sites, and 32 trivalent octahedral sites to maintain a balance between cations and anions in the crystal structure. In the case of spinel ferrite tetrahedral sites, consist of A^{2+} cations, and octahedral sites have Fe^{2+} cations for example Mn_3O_4[3], $ZnFe_2O_4$[4], whereas in inverse spinel ferrite has Fe^{3+} ions distributed between octahedral and tetrahedral sites, while A^{2+} ions occupy only at octahedral, for example, Fe_3O_4[5,6], $NiFe_2O_4$[7], and mixed spinel ferrite has cations that occupy randomly at both sites, for example, $MnFe_2O_4$[8], $MgFe_2O_4$[9]. Spinel ferrites can be constructed to various morphologies by methods including hydrothermal, sol-gel, solvothermal, co-precipitation, ultrasonication, and polyol route[10-14] and they are subjected to wide spread application in catalysis, sensing, supercapacitors, drug delivery, and information storage[15-20].

Ferrites are a class of crystalline compounds, and have gained considerable attention in recent years in the electrochemical sensing of wide variety of analytes. Among the ferrites, the noble metal ferrite, silver ferrite has attracted much research interest, as it is capable of interacting rapidly with many analytes, which is essential for designing of novel electrochemical sensors. As it is semiconducting, for rapid electron capture and transport, an additional is required to be added. For this purpose, graphene oxide (GO) is highly preferred for more than a decade due to its extraordinary surface area and electrical conductivity, simple synthetic route, remarkable electrocatalytic properties, environmentally friendly nature, and unique functionalities[21-24]. Due to its outstanding properties, it is widely used in photocatalysis, sensors, supercapacitors, SERS, membranes, Adsorbents and drug delivery applications. GO can be obtained from natural graphite by oxidation and subsequent exfoliation using the modified hummers method. GO-based sensors are being used for the detection of a wide range of chemicals and biomolecules[25-30]. On chemical modification GO has the ability to act both as chemical and biosensors[31]. Many kinds of research

were focused on the determination and detection of chemicals and biomolecules using GO and its nanocomposites[32-34].

Gallic acid (GA), 3,4,5-trihydroxy benzoic acid, occurs abundantly in plants, and is indispensable for human health. It is an anti-bacterial, anti-oxidant and anti-diabetic, and possess anti-tumor activity. It is a scavenger of free radial and protects human from cardiovascular diseases. It is often used as an indicator to verify the authenticity of fruit juices and alcoholic beverages. In recent years, it has been exploited as adulterant for fake liquors. As GA is in direct control of human metabolism, sensing and quantification of GA in body fluids becomes vital. So in the present study it was planned to apply electrochemical methods like CV and DPV to quantify GA. As these methods are simple, fast, sensitive and cheap. Carbon Paste electrode was used for electrochemical sensing of gallic acid by fabricated Zirconia doped on GO nanocomposite[36]. Polyimide modified platinum electrode was developed by Duran *et al*. for the electrochemical sensing of gallic acid[37]. Madhusudana *et al*. developed bismuth nanoparticle decorated MWCNT as an carbon paste electrode for quantitative determination of GA at neutral *p*H[38]. Capped GA (polyphenol)-Au nanoparticle decorated MWCNT-GO nanocomposite was synthesized for the electrochemical detection[39]. Viswanathan *et al*. developed an ZnO films whose thickness controlled by RFMS technique on FTO substrate using substrate temperature for electrochemical detection of gallic acid[40]. In this work, $AgFe_2O_4$ was blended with GO to form a nanocomposite electrode material for the development of an electrochemical sensor for the detection of gallic acid. Their properties were characterized by FTIR, RAMAN, FESEM, and XRD. To the best of our knowledge, this was the first attempt made to form an $AgFe_2O_4$/GO nanocomposite as an electrode material for the electrochemical detection of gallic acid.

Experimental Section

Graphite powder, sodium nitride ($NaNO_3$) potassium permanganate ($KMnO_4$), sulphuric acid (H_2SO_4), hydrogen peroxide (H_2O_2), hydrochloric acid (HCl), silver nitrate ($AgNO_3$), ferric chloride hexahydrate ($FeCl_3.6H_2O$), lithium triethylborohydride (super hydride)were purchased from Sigma -Aldrich and doubly distilled(DD) water were used throughout the work.

Preparation of graphene oxide

Graphene oxide(GO) was prepared from graphite by the modified hummers method. Graphite powder (2g) and sodium nitride were allowed to stir together by the addition of 40 mL of sulphuric acid in a 1 L round bottom flask for 2 h at 0°C. Then 6g $KMnO_4$ was added to the contents under vigorous stirring and the temperature was maintained at 15°C. Later the ice bath was removed and allowed to stir at room temperature for 2 h. The contents were diluted by the addition of 200 mL of DD water and the temperature was increased to 90°C, and allowed to stir for an hour. After which the contents were added with 10 mL of fresh H_2O_2 to terminate the reaction. The mixture was centrifuged using 8% HCl and the precipitate was dried at 85°C for 24 h.

Preparation of $AgFe_2O_4$ /GO nanocomposite

$AgFe_2O_4$ /GO was prepared by the stirring and ultrasonic reduction technique. Briefly, 0.03 mmol of $AgNO_3$, 0.03 mmol of $FeCl_3.6H_2O$, and 160 mg of GO were taken in a round bottom flask and the mixture was stirred using a magnetic stirrer followed by ultrasonication (Scheme 1). The resulting

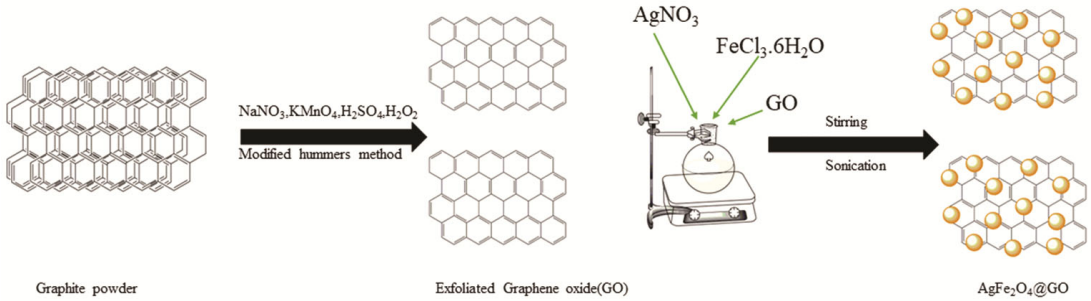

Scheme 1 — Synthesis of $AgFe_2O_4$/GO.

homogenized mixture was then refluxed at 70°C for 150 min. The ions present in the mixture were reduced using super hydride. After cooling to room temperature the contents were centrifuged by washing with DD water and the contents were dried at 80°C in an oven for 40 min. At the same reaction condition, $AgFe_2O_4$ was synthesized without GO for comparison.

Fabrication of $AgFe_2O_4$/GO coated GCE

Previously synthesized nanocomposite (1mg/ 1mL) was dispersed in ethanol. Then the dispersed solution of about 10 µL was drop casted on the surface of GCE and dried at room temperature to obtain $AgFe_2O_4$/GO modified GCE. Later the electrode was used for the determination of gallic acid using CV and DPV. The stock solution of GA was prepared in 0.1M PBS buffer at *p*H 7, stored in the refrigerator at 4 °C, diluted, and used on the requirement.

Results and Discussion

XRD analysis

The crystal structure of the silver ferrite embellished graphene oxide was analyzed by x-ray diffraction. The results are shown in Fig. 1. The reflection at 11.6° (2Θ) is due to GO in the nanocomposite, (Fig. 1b), and it is due to the 001 plane. The peaks of silver ferrite were found to be specific and dominant in the composite. The peaks at 31.82°, 35.52°, 39.04°, 40.16°, 43.56°, 53.84°, and 64.62 (2Θ) correspond to (220), (310), (311), (321), (411), (421), and 333, respectively. It matched with the face-centered cubic (fcc) space lattice for silver ferrite. Thus the reflections present in Figs 1(a) and 1(b) confirm the presence of $AgFe_2O_4$ and GO in the composite.

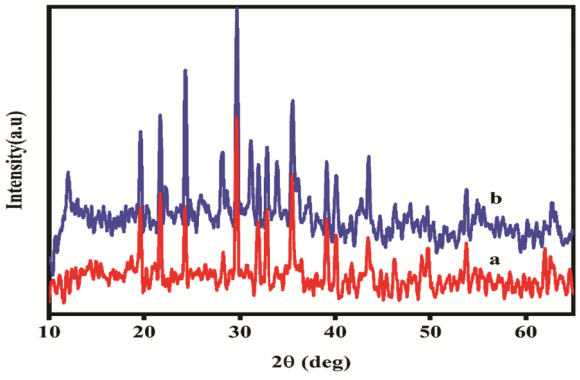

Fig. 1 — X-ray diffraction pattern of (a) $AgFe_2O_4$ and (b) $AgFe_2O_4$/GO.

RAMAN spectral analysis

The Raman spectra of GO, $AgFe_2O_4$ and $AgFe_2O_4$/GO are shown in Fig. 2. There occurred two prominent peaks in both the spectra [Figs 2(a) and 2(c)] due to GO. The intensity of the peaks due to graphene oxide in Fig. 2(c) increased indicating interaction between silver ferrite and GO. The ratio of intensity, I_D/I_G value, increased from 1.16 to 1.68 for pristine GO and $AgFe_2O_4$/GO nanocomposite, respectively. In Fig. 2(b) the peaks at 512 and 688 cm^{-1} represent the presence of Fe-O, and the peaks at 358 cm^{-1} and 1030 cm^{-1} represent Ag functionalization in the composite. The increase in I_D/I_G ratio shows the changes that happened on the surface of GO due to the addition $AgFe_2O_4$.

FTIR analysis

The FTIR spectrum of GO, $AgFe_2O_4$ and $AgFe_2O_4$/GO are shown in Fig. 3. The FTIR presents

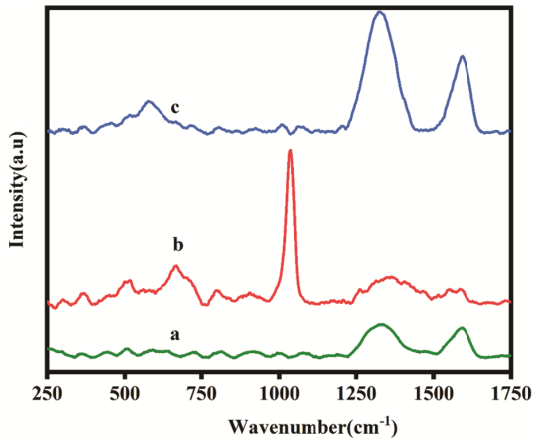

Fig. 2 — RAMAN spectrum of (a) GO; (b) $AgFe_2O_4$ and (c) $AgFe_2O_4$/GO.

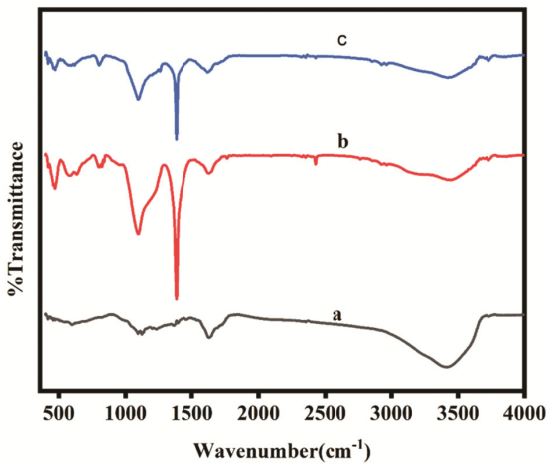

Fig. 3 — FTIR spectrum of (a) GO; (b) $AgFe_2O_4$ and (c) $AgFe_2O_4$/GO.

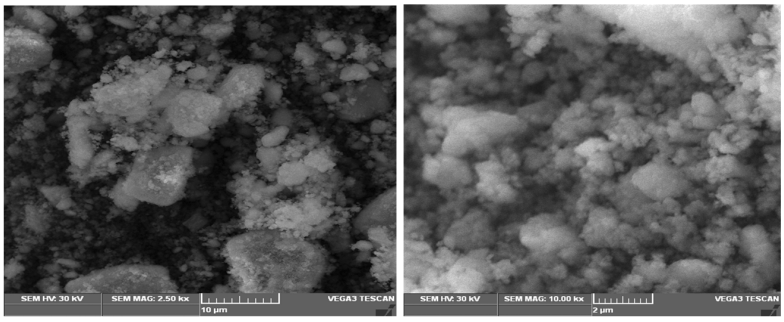

Fig. 4 — Scanning electron microscopic image of $AgFe_2O_4$/GO.

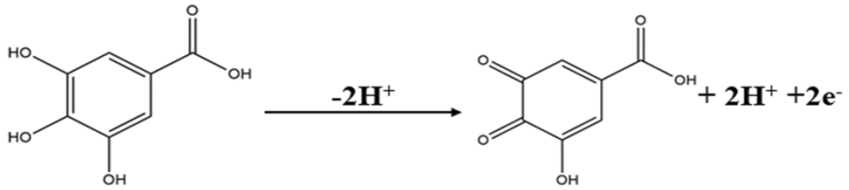

Scheme 2 — Oxidation reaction of GA.

the characteristic peaks of GO at 3412 cm^{-1} and 1612 cm^{-1} corresponding to the presence of -OH stretching vibration and -C=C- stretching vibration respectively. Figures 3b and 3c showed peaks at 1093 cm^{-1} due to Ag-O vibration and at 810 cm^{-1} due to Fe-O vibration. The characteristic peaks of OH stretching vibration and -C=C- stretching vibration occurred at 3446 cm^{-1} and 1640 cm^{-1}. These results confirmed the formation of $AgFe_2O_4$/GO nanocomposite

SEM analysis

The SEM image shows the morphology of the synthesized nanocomposite (Fig. 4). Appearance of white spots on GO is clearly evident from Fig. 4. The average size of the $AgFe_2O_4$ on GO was found to be around 60-90 nm.

TGA analysis

The results of TGA are shown in Fig. 5. The initial weight loss from 25-100°C is due to desorption of water. The sharp weight loss between 150°C and 250°C is due to the degradation of graphene oxide. It was also followed by a final weight loss at 450 °C.

Electrochemical detection of gallic acid

Gallic acid is a natural polyphenol that exists tea leaves, grapes, berries, and many natural products. GA is industrially important due to its application as an antioxidant, anticancer, antidepressant, antiviral, and antibacterial and is also used as an additive in food industries. In this study the electrochemical

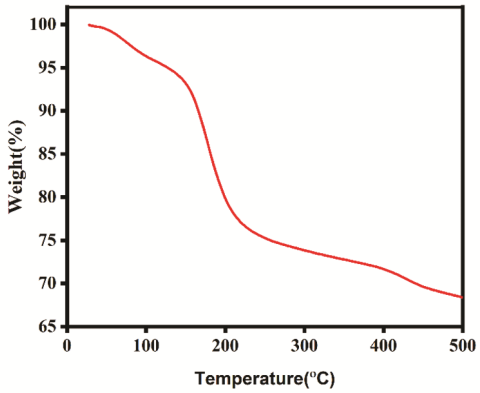

Fig. 5 — Thermal gravimetric analysis of $AgFe_2O_4$/GO.

study was applied to sense gallic acid in aqueous using $AgFe_2O_4$/GO modified glassy carbon electrode (GCE). Both cyclic voltammetric (CV) and Differential pulse voltammetry (DPV) were applied at different *p*Hs ranging from 5.8 to 8.4 maintained with phosphate-buffered saline (PBS). Electrochemical oxidation mechanism of gallic acid at $AgFe_2O_4$/GO modified glassy carbon electrode (GCE) is presented in Scheme 2.

Optimization of modified electrode $AgFe_2O_4$/GO

Effect of pH

The effect of *p*Hs (5.8-8.4) on the electrochemical behavior of gallic acid was studied using $AgFe_2O_4$/GO GCE. The oxidation potential increased with an increase in *p*H from 5.8 to 8.4. As shown in Fig. 6a, at *p*H 7 high current was observed

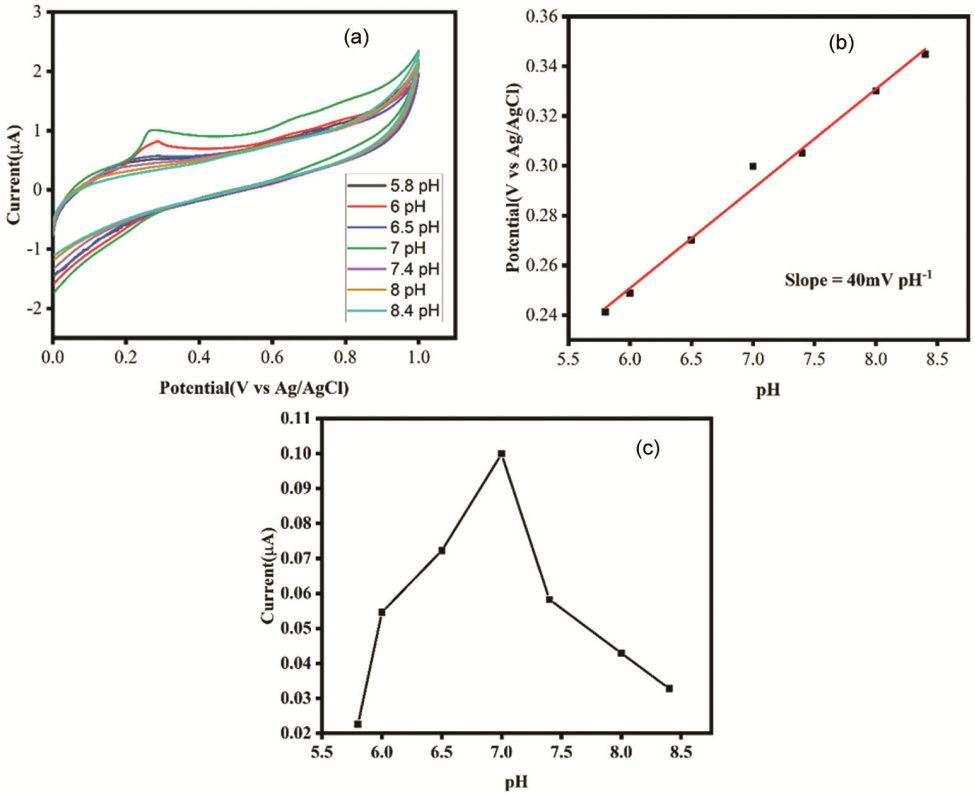

Fig. 6 — (a) Cyclic voltammograms of oxidations of GA in 0.1M PBS at different *p*H with $AgFe_2O_4$/GO/GCE; (b) Plot of *p*H versus potential and (c) plot of *p*H versus current.

at a low potential of 0.29V. The *p*Ka of gallic acid is around 4.5 corresponding to -COOH group and 10 for phenolic -OH group. As the point of zero charge of $AgFe_2O_4$ is around 8.5, its surface is positive below *p*H 8.5 and negative above this *p*H. As at the *p*H 7, GA is negative due to ionization of the -COOH group, it will be easily adsorbed on the positive surface of $AgFe_2O_4$ and get oxidised. So, at the *p*H 7.0, an increase in the current was observed. The Nernstian slope of 40 mV confirms that the reaction proceeds with an unequal number of protons and electron which can be known from Fig. 6b. The anodic peak potential shifted towards the negative value with the increase in *p*H. The plot of Epa versus *p*H in 0.1M PBS obtained a linear regression equation (1).

$$E_0^{1/2}(mV) = 40+0.010816 \text{ (correlation coefficient } \gamma=0.9898) \quad \ldots(1)$$

Before the study of the effect of *p*H, the Electrochemical performance of $AgFe_2O_4$/GO was studied in the absence and the presence of 1mM GA at a scan rate of 50 mVs^{-1} using PBS 0.1M at *p*H 7. The results in the cyclic voltammogram are shown in Fig. 7. In the absence of analyte no peak current was observed for the electrode but for the presence of GA a sharp increase in peak current at a potential of 0.26 V was observed and so the electrode is verified as active for sensing gallic acid.

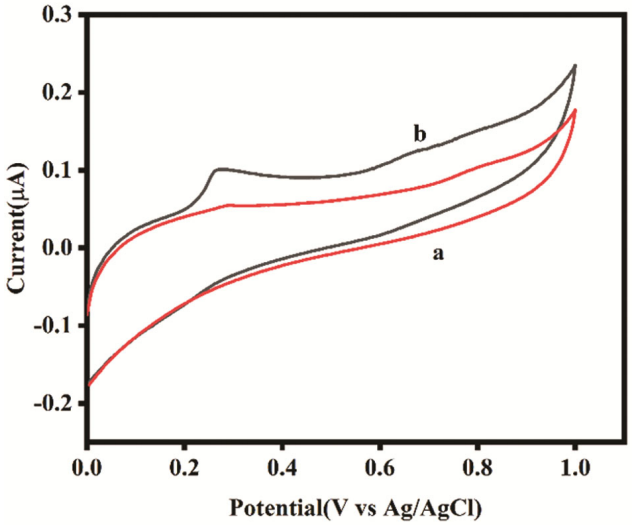

Fig. 7 — Cyclic voltammograms of (a) $AgFe_2O_4$/GO/GCE and (b) 1mM GA at $AgFe_2O_4$/GO/GCE. [Scan rate: 50mV/s (PBS=0.1M, *p*H=7)].

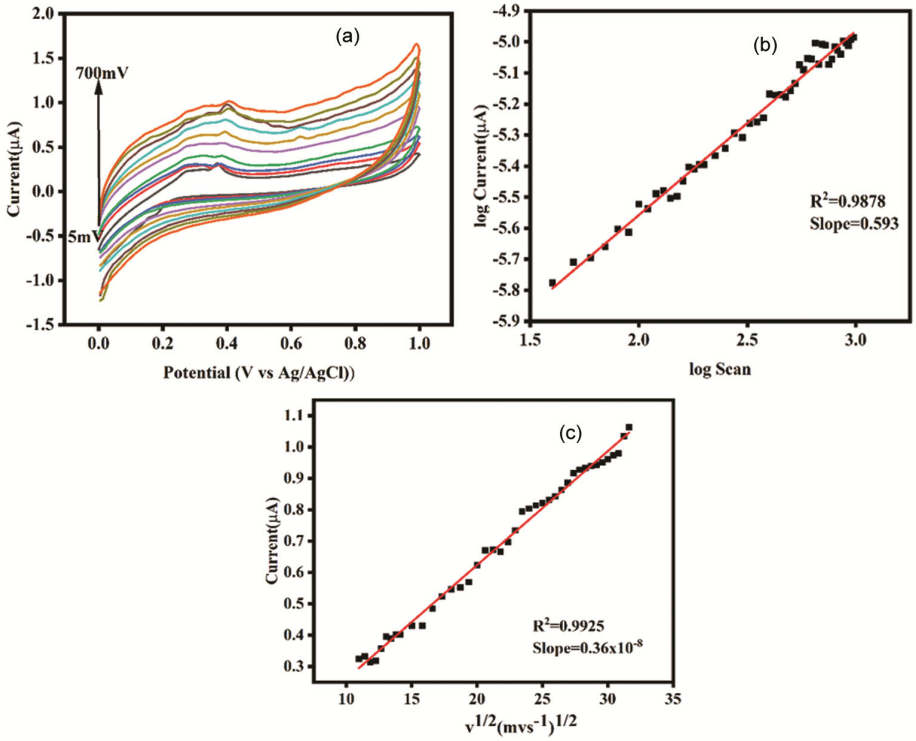

Fig. 8 — (a) Cyclic voltammograms for the oxidation of gallic acid at 0.1M PBS, *p*H-7; (b) Plot of log scan versus log current and (c) Plot of square root of scan rate versus current.

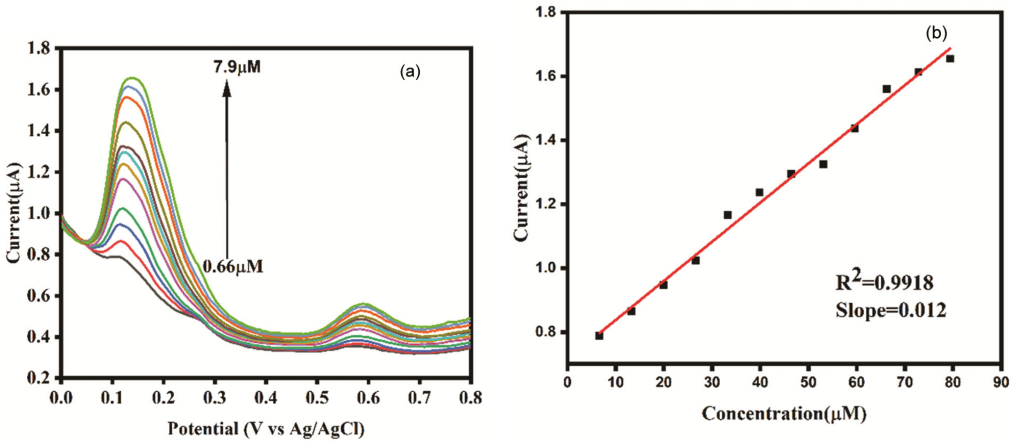

Fig. 9 — (a) Differential pulse voltammogram of oxidation of GA in 0.1M PBS with $AgFe_2O_4$/GO at different concentrations at a scan rate of 50mVs^{-1} and (b) Calibration plot for a concentration of GA versus current.

Effect of scan rate

The effect of scan rate on the electrochemical behavior of GA on $AgFe_2O_4$/GO /GCE was studied from 5 to 700mV s^{-1} and the results are shown in Fig. 8a. The linear calibration graph (a) showed that the anodic peak current value (Ipa) increased as the scan rate increased. The linear relation between log scan rate and log Ip is shown in Fig. 8b. The linear relation between Ipa and the square root of the scan rate is shown in Fig. 8c. These results illustrate the process is adsorption controlled. The double algorithmic plot in Fig. 8c shows the linear relationship that exists between the square root of scan rate and current (Eq. 2).

$$Ipa = 0.36 \times 10^{-8} (v1/2) + 2.975 \times 10^{-6} (R^2 = 0.9925) \quad \ldots (2)$$

Differential pulse voltammogram (DPV)

In differential pulse voltammetry, the sensitivity of $AgFe_2O_4$/GO was determined for the detection of GA Fig. 9. Differential pulse voltammogram curves with

$AgFe_2O_4$/GO GCE for 1mM gallic acid in PBS buffer at *p*H 7 were obtained Fig. 9a. The oxidation current increased on increasing the concentration of gallic acid in a linear concentration range of 0.66-7.9µM along with a LOD of 6.747µM. The limit of quantification (LOQ) was obtained as 22µM with a sensitivity of 0.01µA/µM.

Conclusion

$AgFe_2O_4$ has embellished on GO by simple ultrasonication and stirring method. The synthesized nanocomposite has used to modify the GC electrode for the electrochemical detection of gallic acid. Through linear regression equation, the R^2 and slope values have found to be 0.9878 and 0.593 respectively, which tells that the oxidation of GA proceeds through adsorption controlled process. The modified electrode has shown a range between 0.6 and 7.9µM. Therefore, the fabricated electrode can be extended to electrochemical sensing of more chemical and biological samples, which are also industrially important.

Acknowledgement

The authors are grateful for the financial support provided by Rashtriya Uchchatar Shiksha Abhiyan (RUSA) 2.0 RI & QI and University Research Fellowship (URF).

References

1 Rashad M M, Mohamed R M, Ibrahim M A, Ismail L F M & Abdel-Aal E A, *Adva Powder Technol*, 23 (2012) 315.
2 Ajroudia L, Mlikia N, Bessaisb L, Madigouc V, Villainc S & Leroux Ch, *Mater Res Bull*, 14 (2014) 00351.
3 Jingjing Duan, Sheng Chen, Sheng Dai & Shi Zhang Qiao, *Adv Funct Mater*, 24 (2014) 2072.
4 Peizhi Guo, Lijun Cui, Yiqian Wang, Meng Lv, Baoyan Wang & Xiu Song Zhao, *Langmuir*, 27 (2013) 13189.
5 Yan Wei, Bing Han, Xiaoyang Hu, Yuanhua Lin, Xinzhi Wang & Xuliang Deng, *Proced Eng*, 27 (2012) 632.
6 Murugan E, Nimita J, Ariraman M, Rajendran S, Kathirvel J, Akshata C R & Kumar K, *ACS Omega*, 3 (2018) 13685.
7 Sivakumar P, Ramesh R, Ramanand A, Ponnusamy S & Muthamizhchelvan C, *J Alloys Comp*, 563 (2013) 6.
8 Neda Akhlaghi & Ghasem Najafpour-Darzi, *J Indust Eng Chem*, 103 (2021) 292.
9 Yue Pan, Ying Zhang, Xiaopei Wei, Congli Yuan, Jinling Yin, Dianxue Cao & Guiling Wang, *Electrochim Acta*, 109 (2013) 89.
10 Slimani Y, Almessiere M A, Demir Korkmaz A, Guner S, Güngüneş H, Sertkol M, Yildiz Manikandan A, Akhtar S, Shirsath Sagar E & Baykal A, *Ultrason Sonochem*, 59 (2019) 104757.
11 Zhenxing Yue, Wenyu Guo, Ji Zhou, Zhilun Gui & Longtu Li, *J Magn Magn Mater*, 270 (2004) 216.
12 Shafi Kurikka V P M, Yuri Koltypi, Aharon Gedanken, Ruslan Prozorov, Judit Balogh, Janos Lendvai & Israel Felner, *J Phys Chem B*, 101 (1997) 6409.
13 Stefano Diodati, Luciano Pandolfo, Andrea Caneschi, Stefano Gialanella & Silvia Gross, *Nanoresearch*, 7 (2014) 1027.
14 Guo-Qiang Tan, Yu-Qin Zheng, Hong-Yan Miao, Ao Xia & Hui-Jun Ren, *J Am Ceram Soc*, 95 (2012) 280.
15 Tsoncheva T, Manova E, Velinov N, Paneva D, Popova M, Kunev B, Tenchev K & Mitov I, *Catal Commun*, 12 (2010) 105.
16 Panpan Zhang, Hongwei Qin, Wei Lv, Heng Zhang & Jifan Hu, *Sens Actuat* B, 246 (2017) 9.
17 Sharma R, Thakur P, Sharma P & Sharma Vineet, *J Alloys Comp*, 2017 (17) 30429.
18 Gunjakar J L, *Appl Surf Sci*, 254 (2008) 5844.
19 Manjura Hoque S, Sazzad Hossain Md., Choudhury Shamima, Akhter S & Hyder F, 15 (2015) 30576.
20 Vignesh V, Subramani K, Sathish M & Navamathavan R, *Colloids Surf A*, 538 (2018) 668.
21 Jaemyung Kim, Laura J Cote, Franklin Kim, Wa Yuan, Kenneth R Shull & Jiaxing Huang, *J Am Chem Soc*, 132 (2010) 8180.
22 Ming Zhou, Yueming Zhai & Shaojun Dong, *Anal Chem*, 81 (2009) 5603.
23 Smith Andrew T, La Chance Anna Marie, Zeng Songshan, Liu Bin & Sun Luyi, *Nanomater Sci*, 1 (2019) 31.
24 Murugan E, Govindaraju S & Santhoshkumar S, *Electrochim Acta*, 392 (2021) 138973.
25 Gulsah Yildiz, Majbritt Bolton-Warberg & Firas Awaja, *Acta Biomater*, 131 (2021) 62.
26 Sharma Neeru, Sharma Vikas, Jain Yachana, Kumari Mitlesh, Gupta Ragini, Sharma S K & Sachdev K, *Macromol Symp*, 376 (2017) 1700006.
27 Jieon Lee, Jungho Kim, Seongchan Kima & Dal-Hee Min, *Adv Drug Deliv Rev*, 105 (2016) 275.
28 Murugan E, Akshata C R, Yogaraj V, Sudhandiran G & Babu D, *Ceram Int*, 48 (2022) 16000.
29 Murugan E, Priya A R J, Raman K J, Kalpana K, Akshata C R, Kumar S S & Govindaraju S, *J Nanosci Nanotechnol*, 19 (2019) 7596.
30 Murugan E, Saranya S, Janakiraman K & Greeshma Caroline Titus, *IJ Chem Technol*, 28 (2021) 572.
31 Siva A & Murugan E, *Synthesis*, 17 (2005) 2927.
32 Murugan E & Rangasamy R, *J Biomed Nanotechnol*, 7 (2011) 225.
33 Yogaraj V, Gowtham G, Akshata C R, Manikandan R, Murugan E & Arumugam M, *J Drug Deliv Sci Technol*, 58 (2020) 101785.
34 Murugan E & Vimala G, *J Colloid Interf Sci*, 357 (2011) 354.
35 Murugan E & Shanmugam P, *J Nanosci Nanotechnol*, 16 (2016) 426.
36 Masoud Ghaani, Navid Nasirizadeh, Seyed Ali Yasini Ardakani, Farzaneh Zare Mehrjardi, Matteo Scampicchio & Stefano Farris, *J Anal Meth*, 1 (2013) 1.
37 Chikere Chrys O, Haque Faisal Nadimul, Kong-Thoo-Lin Paul & Fernandez Carlos, *Nanomaterials*, 10 (2020) 537.
38 Aziz Paşahan, Nurcan Ayhan, Imren Ozcan, Serap Titretir Duran & Süleyman Koytepe, *Polym-Plast Technol Eng*, 58 (2019) 1525.